Shaw, E. (1970), *Physiol. Rev. 50*, 244.
Singer, S. J. (1967), *Advan. Protein Chem. 22*, 1.
Sporn, M. B., Berkowitz, D. M., Glinski, R. P., Ash, A. B., and Stevens, C. L. (1969a), *Science 164*, 1408.
Sporn, M. B., Lazarus, H. M., Smith, J. M., and Henderson, W. R. (1969b), *Biochemistry 8*, 1698.
Turner, A. F., and Khorana, H. G. (1959), *J. Amer. Chem. Soc. 81*, 4651.
Ukita, T., and Hayatsu, H. (1962), *J. Amer. Chem. Soc. 84*, 1879.
Wofsy, L., Metzger, H. M., and Singer, S. J. (1962), *Biochemistry 1*, 1031.

Mie Scattering by Optically Active Particles*

David J. Gordon

ABSTRACT: A method, based on classical Mie theory, is presented for calculating the effects of scattering on the circular dichroism (CD) and optical rotatory dispersion (ORD) of suspensions of optically active spherical particles. The method is illustrated for model solid spheres with the known intrinsic optical constants of a helical polypeptide. Significant size-dependent effects of two types are predicted in the ultraviolet, CD, and ORD spectra of this model. (1) Unequal scattering of left and right circularly polarized light distorts these spectra and gives rise to substantial red shifts (*e.g.*, 2–3 nm for spheres of radius 0.03 μ). (2) At wavelengths where absorption is high, the CD and ORD spectra exhibit flattening, which is increasingly severe as particle size is increased. Similar significant effects are also predicted for a spherical shell model. Red shifts and distortions similar to those calculated here have been observed experimentally in the CD and ORD of suspensions of biological particles, such as membranes and viruses; scattering is a likely basis of these observed effects.

Ultraviolet circular dichroism (CD)[1] and optical rotatory dispersion (ORD) have been widely applied as structural probes of biological molecules and macromolecules in solution. In the past 5 years, these probes have been extended to particulate systems, such as plasma membranes (Wallach and Zahler, 1966; Lenard and Singer, 1966; Gordon *et al.*, 1969; Glaser *et al.*, 1970), mitochondria (Urry *et al.*, 1967; Steim and Fleischer, 1967; Wrigglesworth and Packer, 1968), and viruses (Maestre and Tinoco, 1967), with the goal of obtaining information about the structure of their component macromolecules. In these studies, models of membrane or virus structure were based on CD and ORD spectra without full appreciation of the potentially significant effect of scattering on these measurements; such effects were either neglected or dismissed on the basis of inadequate experimental tests.

Recent experimental studies (Ji and Urry, 1969; Urry *et al.*, 1970; Schneider *et al.*, 1970) demonstrate that CD and ORD measurements on particulate systems do in fact exhibit substantial dependence on particle size, for sizes comparable to or exceeding the wavelength of light. Such effects distort the CD and ORD spectra and obscure their informational content; from the biologist's point of view, they are therefore artifacts.

Experimental evidence alone is insufficient to unambiguously distinguish information from artifact; for this purpose, a quantitative theoretical understanding of the physical origins of the effect of particle size upon CD and ORD spectra is essential. Previous theoretical calculations of these artifacts (Urry and Ji, 1968; Ottaway and Wetlaufer, 1970; Gordon and Holzwarth, 1971a; Glaser and Singer, 1971) have been based on the absorption flattening formulation of Duysens (1956), in which scattering is neglected, and on Rayleigh scattering theory, which is valid only for particles much smaller than the wavelength of light. As Schneider (1971) has indicated, these treatments also share the fundamental flaw of treating absorption and refraction as independent phenomena, and not as the imaginary and real parts of a single complex analytic function of wavelength. A calculation of the size-dependent artifacts in the CD and ORD, based on classical Mie scattering theory, in which these objections are removed, is presented in the present paper.

In this paper, only suspensions of identical, discrete, optically active, spherically symmetric particles are considered. It is assumed that the suspensions are sufficiently dilute that the waves scattered by individual particles are not coherently related; multiple scattering effects are neglected. A scattering matrix formulation of the Mie theory is applied to this model to derive expressions for CD, ORD, optical density (OD), and refractive index of a suspension from the corresponding intrinsic spectral properties of the scatterers. The relative roles of absorption and scattering in the calculated CD and OD spectra are analyzed. The nature and magnitude of the size-dependent artifacts predicted by the model are illustrated for two simple spherical geometries: (1) the solid sphere, which is perhaps a useful representation of viruses and other solid particles of biological interest, and (2) the spherical shell, which approximates the shape of a solvent-filled membrane vesicle. For the solid sphere, CD, ORD, and OD spectra are calculated for suspensions of several sizes of spheres having the assumed optical properties of a synthetic helical polypeptide; substantial artifacts, not unlike those observed ex-

* From the Department of Chemistry, University of Chicago, Chicago, Illinois 60637. *Received July 19, 1971.* The work reported here was supported by PHS Training Grant HD-00001 from the National Institute of Child Health and Human Development, and by Grant NS-07286 from the National Institute of Neurologic Diseases and Stroke, U. S. Public Health Service.

[1] Abbreviations used are: CD, circular dichroism; ORD, optical rotatory dispersion; OD, optical density; PGA, poly-L-glutamic acid.

perimentally by Urry *et al.* (1970), are predicted. For the spherical shell, the dependence of absorption and scattering on shell radius and complex refractive index is sketched and related to optical activity. Spectral calculations for a membrane system with an assumed shell geometry (Gordon and Holzwarth, 1971b) predict substantial CD and ORD distortions which agree quantitatively with experimental curves. The important computational methods and some sample numerical results are provided in a brief appendix.

Mie Scattering Matrix for Optically Active Spheres

Mie's scattering theory (Mie, 1908; van de Hulst, 1957b; Kerker, 1969a) provides a solution of Maxwell's equations for a spherically symmetric particle in the field of a plane electromagnetic wave. This theory is extended in this section to yield expressions for the changes in intensity and phase of a beam of left or right circularly polarized light transmitted without change in direction by a suspension of optically active, spherically symmetric particles. The differences in intensity and phase between the two polarizations are measured by CD and ORD; the averages of these quantities are measured by OD and refractive index. These changes in intensity and phase of the light transmitted are the result of interference between the incident wave and the waves scattered in the direction of incidence by each particle.

The scattered wave arising from a spherical scatterer in an oscillating electromagnetic field of arbitrary polarization is most conveniently derived in the scattering matrix formalism (van de Hulst, 1957a; Schnieder, 1971). In this formalism the two mutually orthogonal components of the electric (or magnetic) field of the scattered wave orthogonal to its propagation vector are related to the corresponding components of the incident wave by a 2 × 2 complex scattering matrix, **S**, as follows

$$\mathbf{E}^s = \frac{e^{ik(z-r)}}{ikr}\mathbf{S}\mathbf{E}^0 \tag{1}$$

where $\mathbf{E}^s$ and $\mathbf{E}^0$ are the electric field vectors of the scattered and incident waves, z is the propagation coordinate of the incident wave, r is the distance between the point where $\mathbf{E}^s$ is measured and the center of the scatterer, and k is the wave number of the radiation in the suspending medium.

In the absence of optical activity, the scattering plane, defined as the plane which contains the propagation vectors of the incident and scattered waves, is useful in choosing a basis for **S**. If one takes E_1 as the component of **E** in this plane and E_2 as the component orthogonal to this plane, the matrix **S** relating $\mathbf{E}^s$ to $\mathbf{E}^0$ is diagonal and can be written as

$$\mathbf{S}(\psi) = \begin{pmatrix} S_1(\psi) & 0 \\ 0 & S_2(\psi) \end{pmatrix} \tag{2}$$

where ψ is the angle between the propagation vectors of the incident and scattered waves. The Mie theory gives the following expressions for S_1 and S_2 (van de Hulst, 1957b)

$$S_1(\psi) = \sum_{n=1}^{\infty} \frac{2n+1}{n(n+1)} \{a_n\pi_n(\cos\psi) + b_n\tau_n(\cos\psi)\} \tag{3}$$

$$S_2(\psi) = \sum_{n=1}^{\infty} \frac{2n+1}{n(n+1)} \{a_n\tau_n(\cos\psi) + b_n\pi_n(\cos\psi)\} \tag{4}$$

where π_n and τ_n are angular factors containing associated Legendre polynomials, and a_n and b_n are complex coefficients determined by the complex refractive index and detailed geometry (*e.g.*, simple sphere, spherical shell) of the scatterer. How is the polarization of the scattered wave at angle ψ related to that of the incident wave? Due to the nonequality of the complex elements S_1 and S_2 of the diagonal scattering matrix, these polarizations will generally differ, unless the incident wave is polarized in a plane parallel or perpendicular to the scattering plane. However, in the special case of scattering directly forward ($\psi = 0$), in which symmetry precludes the designation of a unique scattering plane, one obtains the simplified result (van de Hulst, 1957b) that

$$S_1(0) = S_2(0) = \frac{1}{2}\sum_{n=1}^{\infty}(2n+1)(a_n + b_n) \equiv S \tag{5}$$

Thus, **S**(0) is a scalar, and there can be no difference in polarization between the incident and forward-scattered waves.

An optically active particle is characterized by two slightly differing complex refractive indices: m_L for left circularly polarized light (L), and m_R for right circularly polarized light (R). Scattering by such a particle is thus most conveniently examined in a new basis set, consisting of the vectors for left and right circular polarization (Schneider, 1971). The transformation to this new basis from that used in the previous paragraph is represented by

$$\begin{pmatrix} E_L \\ E_R \end{pmatrix} = \frac{1}{\sqrt{2}}\begin{pmatrix} 1 & i \\ 1 & -i \end{pmatrix}\begin{pmatrix} E_1 \\ E_2 \end{pmatrix} \tag{6}$$

Let $S_{1L}(\psi)$ and $S_{2L}(\psi)$ indicate the matrix elements in eq 2 calculated from the complex refractive index of the particle for left circularly polarized light; let $S_{1R}(\psi)$ and $S_{2R}(\psi)$ similarly indicate the matrix elements for right circularly polarized light. The scattering matrix $\mathbf{S}_c$ in the new circular basis is then given by

$$\mathbf{S}_c(\psi) = \frac{1}{4}\begin{pmatrix} 2S_{1L}(\psi) + 2S_{2L}(\psi) & S_{1L}(\psi) + S_{1R}(\psi) - S_{2L}(\psi) - S_{2R}(\psi) \\ S_{1L}(\psi) + S_{1R}(\psi) - S_{2L}(\psi) - S_{2R}(\psi) & 2S_{1R}(\psi) + 2S_{2R}(\psi) \end{pmatrix} \tag{7}$$

In general the polarization state of the scattered wave is not simply related to that of the incident wave. However, in the special direction $\psi = 0$, the off-diagonal components of $\mathbf{S}_c$ vanish. This implies that if an incident beam is left or right circularly polarized, the forward-scattered wave is identically polarized. Thus, the circular scattering matrix $\mathbf{S}_c(0)$ in the forward direction assumes the simple form

$$\mathbf{S}_c(0) = \begin{pmatrix} S_L & 0 \\ 0 & S_R \end{pmatrix} \tag{8}$$

where S_L and S_R are defined by eq 5 using the a_n and b_n calculated for left or right circularly polarized light, respectively.

The characteristics of the light beam transmitted by an optically active suspension are readily obtained by adding to the incident wave the scattered wave at $\psi = 0$ derived by this matrix (van de Hulst, 1957b), and multiplying by the number N of particles per unit volume

$$\theta_T = N\pi k^{-2}h\, Re\{S_L - S_R\} \tag{9}$$

$$\phi_T = N\pi k^{-2}h\ Im\{S_L - S_R\} \quad (10)$$

$$A_T = 2N\pi k^{-2}h\ Re\{S_L + S_R\} \quad (11)$$

$$n_T - 1 = N\pi k^{-3} Im\{S_L + S_R\} \quad (12)$$

where θ_T and ϕ_T are the CD and ORD in radians, A_T is the OD in base e, n_T is the refractive index of the suspension divided by that of the solvent, and h is the path length.

Equations 9–12 predict experimentally measurable properties of light passing through a suspension and reaching a detector placed at $\psi = 0$; they contain no information about the portion of the incident light energy which is either absorbed or scattered at some non-zero ψ, and therefore never reaches this detector. However, simple expressions for total scattered intensity of left and right circularly polarized light are readily obtained from the Mie theory by integrating $\mathbf{S}_c(\psi)$ over all ψ. (Symmetry requires that the off-diagonal components of $\mathbf{S}_c$ average to zero in this integration.) All incident light energy not reaching the detector at $\psi = 0$ which is not accounted for by this integrated scattered intensity must be ascribed to absorption.

The resolution of the total CD and OD signals into scattering and absorptive components is conveniently formulated in a slightly modified notation. Let us define normalized cross sections of scattering (σ_S) and absorption (σ_A) as the respective fractions of radiant energy incident on the geometric cross section of a single particle which are scattered at $\psi \neq 0$ or absorbed. The sum of these two cross sections is denoted by σ_T and is termed the total extinction cross section. Mie theory gives the following expressions for σ_T, σ_S, and σ_A (van de Hulst, 1957b)

$$\sigma_T \equiv 4(kR)^{-2}Re\{S\} = 2(kR)^{-2}\sum_{n=1}^{\infty}(2n+1)Re\{a_n + b_n\} \quad (13)$$

$$\sigma_S \equiv 2(kR)^{-2}\sum_{n=1}^{\infty}(2n+1)(|a_n|^2 + |b_n|^2) \quad (14)$$

$$\sigma_A \equiv \sigma_T - \sigma_S \quad (15)$$

where R is the particle radius. The separate contributions of scattering and absorption to the CD (θ_S and θ_A) and OD (A_S and A_A) of an optically active suspension, as well as the total CD (θ_T) and OD (A_T), are compactly expressed in this cross-sectional notation

$$\theta_T = N\pi R^2 h\ (\sigma_{T,L} - \sigma_{T,R})/4 \quad (16)$$

$$\theta_S = N\pi R^2 h\ (\sigma_{S,L} - \sigma_{S,R})/4 \quad (17)$$

$$\theta_A = \theta_T - \theta_S \quad (18)$$

$$A_T = N\pi R^2 h\ (\sigma_{T,L} + \sigma_{T,R})/2 \quad (19)$$

$$A_S = N\pi R^2 h\ (\sigma_{S,L} + \sigma_{S,R})/2 \quad (20)$$

$$A_A = A_T - A_S \quad (21)$$

The results of this section enable one to predict the spectral properties of suspensions of optically active, spherically symmetric particles, provided that their intrinsic optical constants and detailed geometry are known. The Mie cross section of particles consisting of an inner sphere surrounded by a concentric shell may be caluclated from expressions for the scattering coefficients a_n and b_n derived by Aden and Kerker (1951). The application of the Mie theory to two simple examples of this geometry, the solid sphere and the spherical shell, is illustrated in the next two sections.

The Solid Sphere

In order to establish quantitatively the magnitudes of Mie scattering effects upon CD and ORD, the intrinsic optical constants of the scatterer must be known or accurately estimated. Fortunately these constants can often be obtained from solution measurements of absorbance (A_{soln}), refractive index (n_{soln}), circular dichroism (θ_{soln}), and optical rotation (ϕ_{soln}). For a particle of density ρ, the complex refractive indices m_L and m_R for left and right circularly polarized light may be expressed in the following manner from optical measurements on a solution of its components

$$m_L = n_0\left\{1 + \frac{\rho}{c}(n_{soln} - 1) - i\frac{\rho}{2hck}A_{soln} + \frac{\rho}{hck}(\phi_{soln} - i\theta_{soln})\right\} \quad (22)$$

$$m_R = n_0\left\{1 + \frac{\rho}{c}(n_{soln} - 1) - i\frac{\rho}{2hck}A_{soln} - \frac{\rho}{hck}(\phi_{soln} - i\theta_{soln})\right\} \quad (23)$$

where h and c are the path length and concentration of the solution, and n_0 is the refractive index of the solvent. In these equations, ϕ_{soln} and θ_{soln} are expressed in radians, A_{soln} is expressed in base e, and n_{soln} is the real refractive index of the solution divided by that of the solvent.

A model system in which the application of eq 22 and 23 is usefully illustrated is a hypothetical suspension of solid spheres of an α-helical synthetic polypeptide, poly-L-glutamic acid (PGA). This model is of interest for two reasons. First, the ultraviolet optical properties of solutions of helical PGA are similar to those of solutions of natural proteins of substantial α-helical content, such as those found in cellular membranes. Second, aggregation-dependent changes in the ultraviolet CD of solutions of PGA, presumably without conformational changes, have been investigated experimentally by Ji and Urry (1969) and by Urry *et al.* (1970). They found that the CD of the PGA aggregates is shifted to the red by 2–3 nm, and that its amplitude is flattened increasingly severely as one scans to shorter wavelengths; similar features have been observed in the CD of cellular membranes. Thus, theoretical calculations of aggregation-dependent CD changes in PGA may be usefully compared to observed effects in PGA itself and in systems of biological interest.

In order to carry out the Mie calculations on the PGA sphere model, the following values are assigned to the parameters in eq 22 and 23. The optical properties A_{soln}, θ_{soln}, and ϕ_{soln} are taken from published data (Urry *et al.*, 1970; Urry and Krivacic, 1970); these spectra are normalized to h = 0.1 cm and $c = 1.5 \times 10^{-4}$ g/cm^3. It is assumed that ρ = 1.5 g/cm^3 (Urry and Krivacic, 1970). The refractive index, n_0, of the solvent, water, varies smoothly from 1.38 to 1.43 (International Critical Tables, 1930) over the spectral range of interest (240–190 nm); little accuracy is lost by assuming

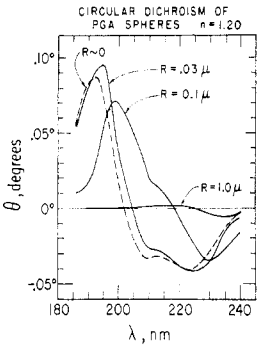

FIGURE 1: Calculated CD of hypothetical suspensions of spheres of helical PGA. The CD of molecularly dissolved PGA ($R \sim 0$), taken from Urry *et al.* (1970), is shown for comparison. All curves shown are for a PGA concentration of 1.5×10^{-4} g/cm^3 and a path length of 0.1 cm. The density of solid PGA is taken to be 1.5 g/cm^3; the solvent refractive index is fixed at 1.4.

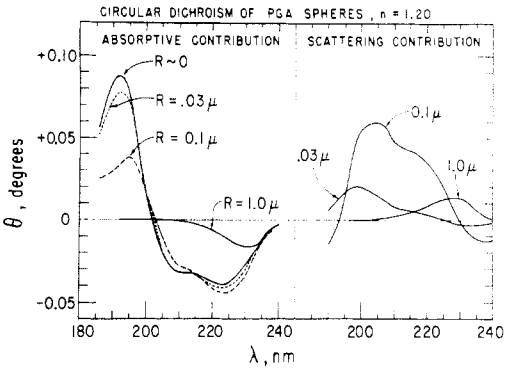

FIGURE 3: Absorptive and scattering contributions to calculated CD of hypothetical suspensions of spheres of helical PGA. The CD of molecularly dissolved PGA ($R \sim 0$), taken from Urry *et al.* (1970), is shown in the left frame for comparison. All curves shown are for a PGA concentration of 1.5×10^{-4} g/cm^3 and a path length of 0.1 cm. The density of solid PGA is taken to be 1.5 g/cm^3; the solvent refractive index is fixed at 1.4.

a constant $n_0 = 1.40$. The refractive index n_{soln} of PGA solutions has not been measured in the ultraviolet spectrum. For simplicity, a constant value of $n \equiv 1 + (\rho/c)(n_{soln} - 1) = 1.20$ is assumed; the consequences of this assumption will be brought out later in the discussion.

Ultraviolet optical activity spectra were calculated by eq 9 and 10 for this model system for three choices of radius. The calculated CD is plotted, along with θ_{soln} ($R \sim$O), *vs.* vacuum wavelength, λ, in Figure 1; the corresponding ORD curves are displayed in Figure 2. The CD and ORD spectra, which are related by Kronig–Kramers transforms (Moffitt and Moscowitz, 1959) at each value of R, exhibit substantial interdependent scattering effects.

The CD and ORD spectra calculated for $R = 0.03\ \mu$ strongly resemble the respective solution spectra. However, it can be seen that the peak and cross-over positions in both spectra of this suspension are consistently red-shifted relative to their positions in the solution curves. Furthermore, the suspension CD and ORD are both somewhat distorted in shape; the enhancement of the long wavelength (225 nm) relative to the short-wavelength (210 nm) CD trough should especially be noted. The calculated CD is similar to that observed experimentally for aggregated PGA by Urry *et al.* (1970), although agreement is not quantitative, especially for λ <200 nm.

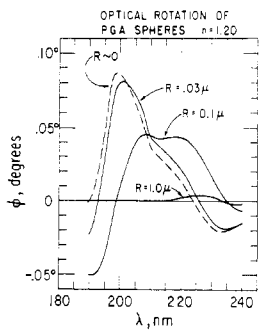

FIGURE 2: Calculated ORD of hypothetical suspensions of spheres of helical PGA. The ORD of molecularly dissolved PGA ($R \sim 0$), taken from Urry and Krivacic (1970), is shown for comparison. All curves shown are for PGA concentration of 1.5×10^{-4} g/cm^3 and a path length of 0.1 cm. The density of solid PGA is taken to be 1.5 g/cm^3; the solvent refractive index is fixed at 1.4.

As the PGA is collected into increasingly larger aggregates, the calculated optical activity spectra change radically in appearance. For $R = 0.1\ \mu$, the calculated CD looks more like the optical rotation ϕ_{soln} of the solution than like θ_{soln}; correspondingly, the calculated ORD resembles $-\theta_{soln}$, rather than ϕ_{soln}. This degree of distortion has been observed by Urry *et al.* (1970) in the CD of aggregated Gramicidin *S*. When R is further increased to 1.0 μ, the CD and ORD are both of extremely low amplitude and bear no obvious resemblance to either solution optical activity curve. Thus, as the degree of aggregation is increased over two orders of magnitude in radius, the predicted CD and ORD of a constant concentration of PGA are distorted, at first mildly, but finally beyond recognition.

What are the relative roles of absorption and scattering in the calculated aggregation-induced changes in the CD (and hence in its transform, the ORD) of helical PGA? One may use eq 17 and 18 to separate the total CD (θ_T) into a CD (θ_A) due to unequal absorption of left and right circularly polarized light and a CD (θ_S) due to unequal scattering of the two polarizations. In Figure 3, θ_A and θ_S for the same three particle radii are plotted *vs.* wavelength.

The calculated θ_A spectra in the left frame of Figure 3 may be described as a series of curves, each resembling the CD of PGA in solution ($R \sim 0$), but increasingly flattened in the region of peptide absorption (peak at 190 nm) as R is made larger. This flattening effect is in qualitative agreement with predictions of absorption statistics (Gordon and Holzwarth, 1971a), based on Duysens' (1956) theory, which neglects the bending of light waves when a particle is encountered. This model predicts that the efficiency of absorptive processes progressively decreases as the absorbers are encountered in increasingly larger and scarcer bunches. It should be noted, however, that the more exact Mie calculations predict that θ_A may actually be slightly enhanced at wavelengths where the absorbance is small, presumably due to bending of light toward the center of the particle.

The θ_S spectra shown in the right frame of Figure 3 change markedly with R. For $R = 0.03\ \mu$, the θ_S curve resembles the ORD of PGA in solution, in qualitative (but not quantitative) agreement with the predictions of a simple Rayleigh model (Ottaway and Wetlaufer, 1970), in which absorption by PGA is neglected. For $R = 0.1\ \mu$, θ_S is much larger, and

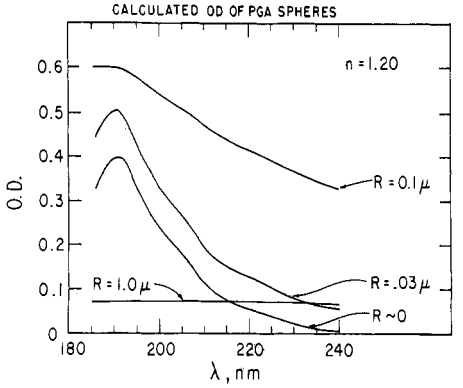

FIGURE 4: Calculated OD (true absorbance + turbidity) of hypothetical suspensions of spheres of helical PGA. The absorbance of molecularly dissolved PGA ($R \sim 0$), taken from Urry *et al.* (1970), is shown for comparison. All curves shown are for a PGA concentration of 1.5×10^{-4} g/cm^3 and a path length of 0.1 cm; OD is in base 10. The density of solid PGA is taken to be 1.5 g/cm^3; the solvent refractive index is fixed at 1.4.

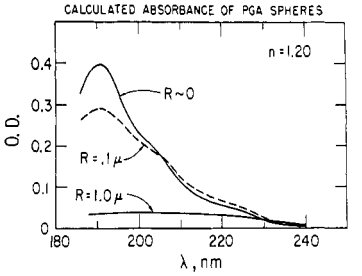

FIGURE 5: Calculated "true" absorbance (base 10) of hypothetical suspensions of spheres of helical PGA. The absorbance of molecularly dissolved PGA ($R \sim 0$), taken from Urry *et al.* (1970), is shown for comparison. All curves shown are for a PGA concentration of 1.5×10^{-4} g/cm^3 and a path length of 0.1 cm. The density of solid PGA is taken to be 1.5 g/cm^3; the solvent refractive index is fixed at 1.4.

there is less likeness to the solution ORD. The calculated θ_S for 1 μ spheres is flattened for similar reasons as θ_A, and bears no resemblance whatever to the ORD of solutions of helical PGA.

The calculated changes in the CD and ORD of helical PGA in varying degrees of aggregation are now understandable. Due to the rough proportionality of θ_A to θ_{soln} (and of the transforms of θ_A and θ_S to ϕ_{soln} and $-\theta_{soln}$, respectively), the CD and ORD of suspensions are both mixtures of the CD and ORD of the solution. The Kronig–Kramers relations require that any single CD band must be accompanied by a biphasic ORD curve which changes sign at the band center. In the long-wavelength (red) wing of the ORD, the CD and ORD have the same sign; in the short-wavelength (blue) wing, they are of opposite signs. Therefore, the intermixture of θ_{soln} and ϕ_{soln} in the CD and ORD of suspensions shifts each CD band and its transform to the red. In addition, amplitude distortions result not only from this intermixture, but also from flattening of θ_A and θ_S (and their transforms); flattening distortions are seen to be especially severe for 1-μ PGA spheres, where $kR \gg 1$.

The mean optical density expected for ideal PGA suspensions of varying particle size can be analyzed under the same set of assumptions by use of eq 19–23. The calculated spectra of A_T (total OD) shown in Figure 4 tend, with the exception of the extreme case ($R = 1.0$ μ), to increase in amplitude at all wavelengths as if from a change in base line, as the particles are made larger. However, even as the optical density increases, the A_T spectra become increasingly featureless with increasing R; for $R = 1.0$ μ, A_T is essentially independent of wavelength. As was the case for CD, the calculated OD curve for $n = 1.20$ and $R = 0.03$ μ fits the observations of Urry *et al.* (1970) for $\lambda > 220$ nm. The semiquantitative agreement of the CD and OD calculated for spheres of 0.03-μ radius with the observed curves for aggregated PGA, suggests that this geometric model may be a good representation of the actual aggregates, subject of course to the validity of our estimate of n.

Again, the separation of absorptive and scattering contributions to the OD is most revealing. The "true" absorbance A_A, plotted *vs.* wavelength in Figure 5, is increasingly depressed in the region where PGA absorbs strongly, as the particles are made larger. This effect is similar to that observed for θ_A in Figure 3 but not as prominent, in accord with the predictions of absorption statistics (Gordon and Holzwarth, 1971a). However, it should be pointed out that A_A, like θ_A, is enhanced where PGA absorbs weakly; this effect is not predicted by theories with neglect scattering.

The scattering term A_S, for which no plots are displayed here, varies little with wavelength at any given R. This featurelessness is only a manifestation of the neglect of refractive index dispersion. This near-constant scattering term is the cause of the apparent "base-line" shifts in A_T; the more meaningful spectral flattening is derived from A_A.

At this juncture it is appropriate to discuss the consequences of the choice of a constant mean real refractive index for the PGA sphere. Refractive index calculations by Urry and Krivacic (1970) for solid PGA, employing the Kronig–Kramers transform of the PGA absorption spectrum and a background term estimated from extrapolation of visible refractive index data of acetic acid and dimethylformamide, indicate a plausible range for the parameter nn_0. From these calculations and the known dispersion of n_0, one may predict that the relative refractive index n varies between 1.2 and 1.35 over the range $190 < \lambda < 240$. In Figures 1–5 we have assumed that $n = 1.20$. A parallel set of curves, calculated with $n = 1.33$, compared in the following manner with those in the figures. The absorptive spectra θ_A and A_A for $n = 1.33$ differed little from those shown for $n = 1.20$. However, the scattering terms θ_S and A_S are changed in a manner similar to the effect of an increase in R. Thus, the net effect of this increase in n is a slightly more distorted CD spectrum (θ_T) and an overall increase in optical density (A_T). If the same curves are calculated for n varying with wavelength between 1.20 and 1.33, the dispersion curve determines the shape of A_S, modifies the shape of θ_S, and affects the θ_A and A_A curves hardly at all. The effect of n on optical density is much greater than on circular dichroism.

The influence of mean real refractive index on these calculations is predictable in a rough qualitative way from the known dependence of the Mie cross sections σ_T, σ_S, and σ_A of spheres on the two parameters kR and m. Calculations for absorbing spheres of varying refractive index show that plots of σ_T *vs.* the single parameter $kR|m - 1|$ are roughly superimposable, provided that $|m - 1| \lesssim 1$ (van de Hulst, 1957c). Thus, a change of refractive index results in a change in σ_T not unlike that due to a change in particle size. A change in $Re\{m\}$ manifests itself primarily through a change in σ_S; a change in $Im\{m\}$ manifests itself primarily through a change in σ_A. The effect of raising n from 1.20 to 1.33 is therefore

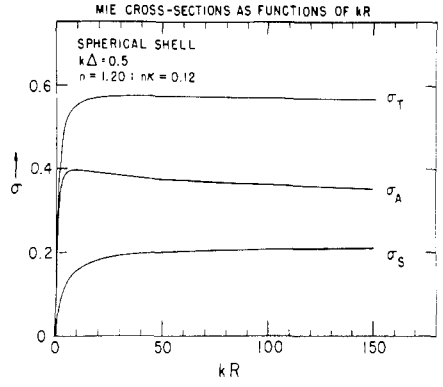

FIGURE 6: Mie cross sections of an optically thin ($k\Delta = 0.5$), absorbing spherical shell as functions of shell radius. A numerical tabulation of these same cross sections is provided in the Appendix as Figure 8.

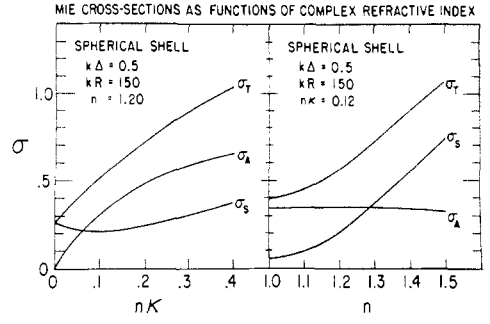

FIGURE 7: Mie cross sections of a large ($kR = 150$), optically thin ($k\Delta = 0.5$) spherical shell as separate functions of imaginary (left frame) and real (right frame) refractive index.

roughly equivalent to that of a 65% increase in kR in the calculation of σ_S.

In addition to the PGA sphere results reported above, preliminary scattering calculations have been carried out for another biologically interesting case, the DNA sphere, in the spectral region 220 nm $< \lambda <$ 320 nm. If one calculates by Mie theory the CD and ORD of a homogeneous sphere of calf thymus DNA (S. Wooley, 1971, unpublished data), with a density of 1 g/cm^3 and an assumed mean real refractive index of 1.20, one obtains red shifts and distortions in both spectra similar to those described for PGA spheres. For $R = 0.05\ \mu$ the CD and ORD bands appear to be red shifted by ≈ 3 nm from their positions in the solution spectra; for $R = 0.10\ \mu$, the red shifts are as great as 10 nm. Thus, scattering effects are likely to play an important role in the CD and ORD of virus particles of dimensions comparable to these. Maestre and Tinoco (1967) have observed in several examples of bacteriophage that the ORD of the intact phage is red shifted relative to the ORD of free DNA, and that these red shifts are eliminated by osmotic lysis of the phage. The observed dependence of these shifts on phage size and the resemblance of the ORD difference curves for intact *vs.* lysed phage to the negative of a CD spectrum of DNA strongly suggest that these shifts may be due (at least in part) to scattering. Red shifts which have been reported by Shih and Fasman (1971) in the CD of nucleohistone complexes may also originate in part or in full from scattering. Although further experimental work is necessary in order to quantitatively delineate the role of scattering in these systems, a note of caution is warranted, nonetheless. One is ill advised to base any hypothesis about local environment in a particulate system upon the observation of aggregation-induced red shifts in CD and ORD, without first allowing for the effects of scattering.

The Spherical Shell

The ultraviolet optical activity of cellular membranes has received much attention during the past 5 years. An easily prepared and frequently studied experimental system is the red blood cell "ghost," in which hemoglobin has been replaced by a transparent solvent. The hollow "biconcave disk" shape of the red cell membrane may be approximated by a spherical shell of thickness $\Delta = 70$ Å and radius $R = 3.5\ \mu$; detailed spectral calculations for this model (Gordon and Holzwarth, 1971b), similar to those of the previous section for PGA spheres, are not reported here. The discussion below is confined to the dependence of σ_T, σ_S, and σ_A for membrane-like spherical shells on size and complex refractive index m; the implications of these considerations for circular dichroism calculations are emphasized. Although optical rotation will not be discussed explicitly, it is implicit that all effects predicted for CD must be accompanied by corresponding effects in its Kronig–Kramers transform, the ORD.

The Mie cross sections of spherical shells are functions of four parameters: $k\Delta$, kR, $n = Re\{m\}/n_0$, and $n_K = -Im\{m\}/n_0$. The shell thickness parameter $k\Delta$ is fixed at 0.5, a reasonable approximation for membranes in the ultraviolet spectrum. The separate dependence of σ_T, σ_S, and σ_A on the remaining three parameters is shown in Figures 6 and 7.

The dependence of the Mie cross-sections on kR for $n = 1.20$ and $n_K = 0.12$ is shown in Figure 6. It can be seen that all three curves have steep positive slopes at small values of kR but level off sharply at high kR. Similar curves for other fixed values of n and n_K all show this type of dependence on kR. Note that this leveling tendency differs from the well-known asymptotic behavior of the cross sections of large solid spheres. For a solid sphere of fixed complex refractive index $m \neq 1$, the cross-section σ_T invariably approaches 2 as $kR \rightarrow \infty$. For spherical shells, the cross-section σ_T also approaches a limit as $kR \rightarrow \infty$, but the limiting value of σ_T depends on the thickness and complex refractive index of the shell. This limiting behavior for spherical shells is due to the fact that when $R \gg \Delta$ and $kR \gg 1$, the shell, over most of its geometric cross section, appears to be two thin scattering surfaces separated by many wavelengths. An increase in radius of such a shell has little effect other than to increase the geometric cross section and to further separate the two surfaces; thus, there is little change in σ_T, σ_S, and σ_A. This relative insensitivity to kR of large shells is useful for spectral calculations on large membranes like the red cell ghost ($kR \cong 150$). Because of this property, statistical distribution of radii and moderate nonsphericity of the shells are likely to be of little significance in suspensions of large membrane vesicles.

The optical activity of suspensions in the Mie model arises from the variations in the calculated cross sections with slight changes in m, as between left (L) and right (R) circular polarization. It is good general assumption that $|m_L - m_R| \ll |m_L + m_R - 2|$; one can therefore write the following Taylor expansions (Schneider, 1971)

$$\sigma_{A,L} - \sigma_{A,R} \cong \frac{\partial \sigma_A}{\partial n}(n_L - n_R) + \frac{\partial \sigma_A}{\partial (n\kappa)}(n_{L\kappa_L} - n_{R\kappa_R}) \quad (24)$$

$$\sigma_{S,L} - \sigma_{S,R} \cong \frac{\partial \sigma_S}{\partial n}(n_L - n_R) + \frac{\partial \sigma_S}{\partial (n\kappa)}(n_L\kappa_L - n_R\kappa_R) \quad (25)$$

The absorptive CD (θ_A) is proportional to $\sigma_{A,L} - \sigma_{A,R}$; the differential scatter (θ_S) is proportional to $\sigma_{S,L} - \sigma_{S,R}$. Thus, θ_A and θ_S are each broken down into a term proportional to the intrinsic ORD ($n_L - n_R$) and another term proportional to the intrinsic CD ($n_L\kappa_L - n_R\kappa_R$) of the shell material. Since the intrinsic shell CD and ORD are of comparable magnitude, the partial derivative coefficients determine the relative weight of these two terms in θ_S and θ_A. By calculating σ_S and σ_A of shells of fixed radius and thickness for several choices of n and $n\kappa$, and then plotting the results, one can display these partial derivatives as functions of n and $n\kappa$; insight can thus be gained into the manner in which the optical activity of a suspension of shells is derived from the optical activity of the shell substance.

Representative plots of σ_A, σ_S, and their sum σ_T for a membrane-like shell ($k\Delta = 0.5$, $kR = 150$) *vs.* $n\kappa$ and *vs.* n are displayed in Figure 7. In the former plot n is fixed at 1.20; in the latter plot $n\kappa$ is fixed at 0.12. One can make the following observations about the partial derivatives in eq 24–25. First, σ_A is quite insensitive to n, and σ_S is quite insensitive to $n\kappa$ over the ranges shown. One then may write that $\partial\sigma_A/\partial n \approx \partial\sigma_S/\partial(n\kappa) \approx 0$. Thus, the intrinsic shell CD dominates the θ_A term of the suspension CD, and the intrinsic shell ORD dominates the θ_S term of the suspension CD. One can also observe in Figure 7 and in similar plots for other fixed values of n and $n\kappa$ that $\partial\sigma_A/\partial(n\kappa)$ decreases with increasing $n\kappa$, and that $\partial\sigma_S/\partial n$ increases as n goes from 1.0 to 1.2 but remains quite constant for $1.2 < n < 1.5$. The former observation is consistent with the absorption flattening arguments previously referred to. The observation that $\partial\sigma_S/\partial n$ does not vary steeply with n facilitates Mie calculations of CD and ORD in suspensions of shells with unknown n. (It must be noted that σ_S itself increases substantially with n, so that, unlike θ_S, the calculated mean turbidity A_S is strongly influenced by choice of n.) Mie cross sections for $k\Delta = 0.5$ and $kR = 150$ were also evaluated for various n with $n\kappa$ fixed at 0.00 and 0.24, and for various $n\kappa$ with n fixed at 1.33. The calculations showed that $\partial\sigma_A/\partial(n\kappa)$ tends to decrease slightly with increasing n and that $\partial\sigma_S/\partial n$ tends to decrease slightly with increasing $n\kappa$.

One may predict from the considerations of this section that the CD of a suspension of large, thin spherical shells is the sum of an absorptive component roughly proportional to the intrinsic CD of the shell substance and a scattering term roughly proportional to the intrinsic shell ORD. Consequently the ORD of such a suspension is the sum of a term (the transform of θ_A) resembling the shell ORD and another term (the transform of θ_S) resembling, but opposite in sign to, the shell CD. The calculated optical activity of large, thin shells is not expected to be strongly sensitive to shell radius or mean real refractive index. These predictions are borne out by calculations on red cell ghost suspensions (Gordon and Holzwarth, 1971b) and are similar to results calculated in the preceding section for small ($R = 0.03\ \mu$) solid spheres.

Conclusions

(1) Application of Mie scattering theory to circularly polarized light yields expressions for CD and ORD, as well as mean OD and refractive index, of suspensions of optically active, spherically symmetric particles. These expressions are readily evaluated for solid spheres and spherical shells. (2) The calculated CD and ORD of suspensions of particles of radius comparable to or greater than $\lambda/2\pi$ differ substantially from the corresponding spectra of a solution of their molecularly dispersed components. However, the Kronig–Kramers transforms relating CD to ORD (and OD to refractive index) are invariant to aggregation. (3) Unequal scattering of left and right circularly polarized light contributes an ORD-like term to the CD of suspensions, and a negative CD-like term to their ORD. Substantial size-dependent red shifts arise from this mixing of CD and ORD in particulate systems. (4) At wavelengths or particle sizes for which the extinction cross section is large, the calculated CD and ORD curves are flattened. Duysens' "absorption flattening" is the qualitative counterpart of this prediction. (5) Red shifts and distortions comparable to those observed experimentally in the CD and ORD of suspensions of biological particles (*e.g.*, red cell ghosts, T2 phage) are calculated by Mie theory for spherical models of these particles. Scattering effects of the sort calculated here are a likely source of these observed anomalies.

MIE CROSS-SECTIONS OF SPHERICAL SHELLS--- K*DELTA=0.5, RE(M)=1.20, IM(M)=-0.12

K*R	SIGMA T	SIGMA S	SIGMA A
1.0	0.30457640	0.03089019	0.27368623
2.0	0.43280852	0.07215643	0.36065209
3.0	0.47894168	0.10270578	0.37623590
4.0	0.50693941	0.11646760	0.39047182
5.0	0.51854348	0.12703151	0.39151192
6.0	0.53224009	0.13852197	0.39371812
7.0	0.54030955	0.14278471	0.39752483
8.0	0.54423505	0.14876479	0.39547020
9.0	0.55064911	0.15417951	0.39646959
10.0	0.55292207	0.15664941	0.39627260
12.0	0.56021744	0.16501755	0.39519989
14.0	0.56333941	0.16997832	0.39336103
16.0	0.56496274	0.17319447	0.39176828
18.0	0.56836718	0.17712116	0.39124596
20.0	0.57027131	0.18056369	0.38970762
25.0	0.57279027	0.18657643	0.38621378
30.0	0.57371330	0.19079536	0.38291788
35.0	0.57461727	0.19395971	0.38065749
40.0	0.57458819	0.19663411	0.37835401
45.0	0.57521582	0.19889694	0.37631881
50.0	0.57491523	0.20082158	0.37409359
100.0	0.57070225	0.20975125	0.36095095
150.0	0.56516677	0.21239841	0.35276830

FIGURE 8: Computer tabulation of Mie cross sections of spherical shells of several radii, with $k\Delta = 0.5$ and $m = 1.20–0.12i$. These data are also displayed graphically in Figure 6.

Appendix

Mie Scattering Computations. The primary object of the Mie theory as applied in this paper is to calculate the cross sections of extinction (σ_T), scattering (σ_S), and absorption (σ_A) of compound spheres (two examples of which are the solid sphere and the spherical shell), from which the circular dichroism and optical density of suspensions of such particles are readily derived. These cross sections were numerically evaluated on a digital computer; double precision (16 significant figures) complex arithmetic was employed. Results obtained by the author's program were checked for accuracy against independent calculations for dielectric spheres (Gumprecht and Sliepcevich, 1951), absorbing spheres (Chromey, 1960), coated dielectric spheres (Kerker *et al.*, 1962), and hollow absorbing shells (L. Battan and B. Herman, 1971, personal communication). In every instance full agreement was obtained. A computer listing of some sample numerical results for hollow absorbing shells is provided in Figure 8.

The Mie cross sections are evaluated by eq 13–15. The complex scattering coefficients a_n and b_n in these equations are ratios of 4×4 determinants containing spherical Bessel functions (j_n), spherical Hankel functions of the second kind (h_n), and their derivatives (Aden and Kerker, 1951; Kerker, 1969b). Although the calculations are mostly straightforward, some features are sufficiently troublesome to warrant discussion. These may be grouped under three headings: (1) evaluation of j_n and h_n, (2) choice of a suitable form for expressing a_n and b_n, and (3) convergence of summations.

(1) The spherical Bessel and Hankel functions obey well-known recursion formulas (Abramowitz and Segun, 1965), upon which their calculation is based. A recursive calculation may be carried forward from low to high orders or backward from high to low orders. In numerical computations of j_n and h_n, where rounding errors are inevitable, the choice of recursion direction is critical. The Bessel function j_n must always be computed by backward recursion; recursion in the forward direction leads to exponential accumulation of error. The choice of recursion direction for h_n depends upon its argument x. When x is real, the real and imaginary parts of $h_n(x)$ must be computed separately; backward recursion is used to compute $Re\{h_n(x)\}$, and forward recursion is used to compute $Im\{h_n(x)\}$. When x is complex, the function $h_n(x)$ is computed by forward recursion. (2) When one is dealing with large absorbing compound spheres, one should avoid the substitution of Neumann functions for Hankel functions in the determinants for a_n and b_n, as in Kerker's (1969b) eq 5.1.27 and 5.1.28. Although a_n and b_n are correctly expressed by the ratios in these equations, the numerators and denominators all approach zero in absorbing particles for which kR and $k(R - \Delta)$ are large. The altered equations are therefore computationally unsuitable in such cases. (3) Convergence of the summations in eq 13–14 is readily obtained to 16 significant figures. Although there is no systematic decreasing tendency in the lower orders of a_n and b_n, the coefficients a_n and b_n decay rapidly with increasing order n when n surpasses kR. Thus, a number of terms not greatly exceeding kR is generally sufficient to give the required convergence.

Acknowledgments

The author thanks Dr. G. Holzwarth for his many valuable contributions to the preparation of this manuscript and to the work reported therein. Thanks are also due to Drs. Louis Battan and Benjamin Herman for helping to check the author's computational accuracy, by providing independent sample calculations of the Mie cross sections of hollow absorbing shells. Ilan Chabay's critical reading of this manuscript is also thankfully acknowledged.

References

Abramowitz, M., and Segun, I. A. (1965), Handbook of Mathematical Functions, New York, N. Y., Dover Publications, Inc.

Aden, A. L., and Kerker, M. (1951), *J. Appl. Phys. 22*, 1242.

Chromey, F. C. (1960), *J. Opt. Soc. Amer. 50*, 730.

Duysens, L. N. M. (1956), *Biochim. Biophys. Acta 19*, 1.

Glaser, M., Simpkins, H., Singer, S. J., Sheetz, M., and Chan, S. I. (1970), *Proc. Nat. Acad. Sci. U. S. 65*, 721.

Glaser, M., and Singer, S. J. (1971), *Biochemistry 10*, 1780.

Gordon, A. S., Wallach, D. F. H., and Strauss, J. H. (1969), *Biochim. Biophys. Acta 183*, 405.

Gordon, D. J., and Holzwarth, G. M. (1971a), *Arch. Biochem. Biophys. 142*, 481.

Gordon, D. J., and Holzwarth, G. (1971b), *Proc. Nat. Acad. Sci. U. S. 68*, 2365.

Gumprecht, R. O., and Sliepcevich, C. M. (1951), Tables of Light Scattering Functions for Spherical Particles, Ann Arbor, Mich., Engineering Research Institute, University of Michigan.

International Critical Tables (1930), Vol. 7, New York, N. Y., McGraw-Hill, p 13.

Ji, T. H., and Urry, D. W. (1969), *Biochem. Biophys. Res. Commun. 34*, 404.

Kerker, M. (1969a), The Scattering of Light and Other Electromagnetic Radiation, New York, N. Y., Academic Press, Chapter 3.

Kerker, M. (1969b), The Scattering of Light and Other Electromagnetic Radiation, New York, N. Y., Academic Press, Chapter 5.

Kerker, M., Kratohvil, J. P., and Matijevic, E. (1962), *J. Opt. Soc. Amer. 52*, 551.

Lenard, J., and Singer, S. J. (1966), *Proc. Nat. Acad. Sci. U. S. 56*, 1828.

Maestre, M. F., and Tinoco, I. (1967), *J. Mol. Biol. 23*, 323.

Mie, G. (1908), *Ann. Physik. 25*, 377.

Moffitt, W., and Moscowitz, A. (1959), *J. Chem. Phys. 30*, 648.

Ottaway, C. A., and Wetlaufer, D. B. (1970), *Arch. Biochem. Biophys. 139*, 257.

Schneider, A. S. (1971), *Chem. Phys. Lett. 8*, 604.

Schneider, A. S., Schneider, M. T., and Rosenheck, K. (1970), *Proc. Nat. Acad. Sci. U. S. 66*, 793.

Shih, T. Y., and Fasman, G. D. (1971), *Biochemistry 10*, 1675.

Steim, J. M., and Fleischer, S. (1967), *Proc. Nat. Acad. Sci. U. S. 58*, 1292.

Urry, D. W., Hinners, T. A., and Masotti, L. (1970), *Arch. Biochem. Biophys. 137*, 214.

Urry, D. W., and Ji, T. H. (1968), *Arch. Biochem. Biophys. 128*, 802.

Urry, D. W., and Krivacic, J. (1970), *Proc. Nat. Acad. Sci. U. S. 65*, 845.

Urry, D. W., Mednicks, N., and Bejnarowicz, E. (1967), *Proc. Nat. Acad. Sci. U. S. 57*, 1043.

van de Hulst, H. C. (1957a), Light Scattering by Small Particles, New York, N. Y., Wiley, Chapter 5.

van de Hulst, H. C. (1957b), Light Scattering by Small Particles, New York, N. Y., Wiley, Chapter 9.

van de Hulst, H. C. (1957c), Light Scattering by Small Particles, New York, N. Y., Wiley, Chapter 11.

Wallach, D. F. H., and Zahler, P. H. (1966), *Proc. Nat. Acad. Sci. U. S. 56*, 1552.

Wrigglesworth, J. M., and Packer, I. (1968), *Arch. Biochem. Biophys. 128*, 790.